Published in final edited form as:
Oncogene. 2009 November 5; 28(44): 3880–3891. doi:10.1038/onc.2009.242.

Anti-cancer DNA Intercalators cause p53 Dependent Mitochondrial DNA Nucleoid Re-modelling

Neil Ashley and **Joanna Poulton**
Nuffield Department of Obstetrics and Gynaecology, University of Oxford, Level 3, Women's Centre, John Radcliffe Hospital, Headington, Oxford, OX3 9DU, United Kingdom

Abstract

Many anti-cancer drugs, such doxorubicin (DXR), intercalate into nuclear DNA of cancer cells thereby inhibiting their growth. However, it is not well understood how such drugs interact with mitochondrial DNA (mtDNA). Using cell and molecular studies of cultured cells we show that DXR and other DNA intercalators such as ethidium bromide, can rapidly intercalate into mtDNA within living cells, causing aggregation of mtDNA nucleoids and altering the distribution of nucleoid proteins. Remodelled nucleoids excluded DXR and maintained mtDNA synthesis, whereas non-remodelled nucleoids became heavily intercalated with DXR, which inhibited their replication leading to mtDNA depletion. Remodelling was accompanied by extensive mitochondrial elongation or interconnection, and was suppressed in cells lacking MFN 1 and OPA1, key proteins for mitochondrial dynamics. In contrast, remodelling was significantly increased by p53 or ATM inhibition, indicating a link between nucleoid dynamics and the genomic DNA damage response.

Collectively, our results show that DNA intercalators can trigger a common mitochondrial response, which likely contributes to the marked clinical toxicity associated with these drugs.

Keywords

Anthracyclines; mtDNA; mitochondria; nucleoids; doxorubicin; ethidium; Mitofusin; OPA1; TFAM; DRP1

Introduction

DNA intercalating drugs form the cornerstone of many anti-cancer regimes. Prominent amongst these are the anthracyclines, a group of compounds including DXR and daunorubicin (Hande, 1998). DNA intercalators function by inserting between the base pairs of the DNA double helix, thereby altering its molecular topology. Consequently, DNA polymerases and other DNA related proteins are inhibited and DNA replication is reduced, causing the death of rapidly dividing cancer cells. Unfortunately anthracyclines can cause severe cardiotoxicity (Singal and Iliskovic, 1998), often manifesting months or even years after treatment (Steinherz and Steinherz, 1991). The reason for this delayed toxicity remains

*Corresponding authors: Neil.Ashley@clin-pharm.ox.ac.uk, Joanna.Poulton@obs-gyn.ox.ac.uk, Tel: 01865 222945, Fax: 01865 769141.

Europe PMC Funders Author Manuscripts

unknown, but one possibility is that anthracyclines induce a lesion capable of damaging the cell over a long period. A potential candidate for such a lesion is the mitochondrion, as cardiac specific mitochondrial dysfunction is an early and specific feature of anthracycline cardiotoxicity (Conklin, 2005; Jung and Reszka, 2001; Tokarska-Schlattner *et al.*, 2006; Wallace, 2003), which can persist even after drug cessation (Zhou *et al.*, 2001). Mitochondria contain a 16.5kb multi-copy genome known as mitochondrial DNA (mtDNA), and extensive mtDNA damage in the form of depletion and deletions has been found in cardiac tissue of DXR treated patients (Lebrecht *et al.*, 2005), as well as rodent and cell culture models (Cullinane *et al.*, 2000; Lebrecht *et al.*, 2004; Suliman *et al.*, 2007). Using the fluorescent DNA dye PicoGreen, that we have previously shown labels specifically nuclear and mtDNA within living cells (Ashley *et al.*, 2005; Ashley *et al.*, 2008), we recently demonstrated that anthracyclines are capable of rapidly penetrating into mitochondria to directly intercalate into mtDNA (Ashley and Poulton, 2009).

In vivo, mtDNA is arranged into punctate nucleoid structures (Garrido *et al.*, 2003; Legros *et al.*, 2004), which consist of several copies of mtDNA bound to ‘nucleoid’ proteins such mtSSB, TFAM and POLG. Although the functional significance of nucleoids remains obscure, yeast nucleoids can undergo structural remodelling in response to metabolic stress in order to protect mtDNA from damage (Chen *et al.*, 2005b; Kucej *et al.*, 2008). Loss of the TFAM homologue and nucleoid protein Abf2p sensitises yeast mtDNA to damage by the DNA intercalator ethidium bromide (Chen *et al.*, 2005b). Within human cells, the tumour suppressor p53 can translocate to mitochondria and interact with POLG in order to protect mtDNA from damage by ethidium bromide (Achanta *et al.*, 2005).

Mitochondria are dynamic organelles which can undergo rapid transient fission and fusion, mediated by pro-fusion proteins such as OPA1 and Mitofusins 1/2, and pro-fission proteins such as DRP1 (Chen *et al.*, 2005a). Recently the anticancer DNA intercalator actinomycin D has been shown to trigger OPA1 and MFN1 mediated stress induced mitochondrial hyperfusion (SIMH), which has a protective anti-apoptotic effect within cells (Tondera *et al.*, 2009). Collectively this evidence suggests that mitochondria and mtDNA may undergo a coordinated stress response in the presence of DNA intercalating drugs.

In this study we sought to study the effects of anti-cancer DNA intercalating drugs on mtDNA and mitochondria. We show that anthracyclines can directly interact with mtDNA at clinically relevant concentrations, producing major alterations of nucleoids and mitochondrial morphology and ultimately resulting in the depletion of mtDNA.

Experimental Procedures

Materials

All chemicals were from Sigma-Aldrich, Axxora or Invitrogen. Antibodies to β-actin, cytochrome c, p53, POLG and TID1 were from Thermo-Fisher, anti-TFAM was raised in our own lab. Anti-DNA (IgM1) was from ProGen Biotechnick, or a kind gift of Peter Cook (IgM2). Anti-BrdU was from Roche. Anti-mtSSB, Anti-ATAD3 and Ditercalinium were generous gifts from Prof. Zeviani, Dr. I. Holt and Prof. B.P. Roques, respectively. MFN1/2 (Chen *et al.*, 2003) and POLG exonuclease null (Trifunovic *et al.*, 2004) mouse embryonic

fibroblasts (MEFs) were the generous gift of Dr. D. Chan and Dr. A. Trifunovic, respectively.

Cell culture and drug treatment

Mycoplasma free normal human fibroblasts, H9C2 rat cardiomyocytes, RH30 and A549 cells were cultured as previously (Ashley *et al.*, 2005). For drug treatments cells were seeded at ~$2 \times 10^6/cm^2$ in dishes and allowed to attach overnight before exposure to 1 ml of drug/vehicle medium per cm^2 of vessel surface area.

Cytochemical labelling

Immuno-cytochemical labelling, histochemical staining of cytochrome c oxidase (COX) activity, bromodeoxyuridine (brdU) labelling of newly synthesised DNA, and PicoGreen labelling were performed as described previously (Ashley *et al.*, 2005). TMRM co-staining was done using 30 nM for 20 minutes. Cells were visualised using a Leica DMI50 microscope fitted with a Hamamatsu ORCA-II camera.

Propidium Iodide/ calcein-AM determination of viability

Cells were incubated with 1 μM calcein-AM and 0.5 μg/ml propidium iodide for 10 minutes and analysed by microscopy.

TUNEL labelling

Detection of methanol fixed apoptotic cells was done using a kit from Takara Bio Inc. (Shigo, Japan).

Digital image analysis

SimplePCI 6 was used for image capture. Image analysis was performed on unprocessed, 8-bit digital images using ImageJ. Fluorescent intensities (pixel grey values) of defined regions of interest (nuclei or nucleoids), corrected for cellular background, were determined as described (Abramoff, 2004). Cell counts where done by manually counting cells from randomly acquired images.

Real-time quantitative PCR

Determination of relative mtDNA to nDNA was performed as described previously (Ashley *et al.*, 2005), except the nuclear probe was labelled with Vic at the 5’ end and amplifications were done simultaneously using a GeneAmp 7700 sequence detection system.

Oxygen consumption

Cells were harvested, counted with a haemocytometer and re-suspended in DMEM without serum or glucose, at 5×10^6 cells/ml. Oxygen consumption was performed on whole cells at 37°C, using a Hansatech Clarke type oxygen electrode.

ATP measurements

Cells were harvested and counted using a haemocytometer and ATP measured using a Promega CellTiter-Glo assay as per manufacturer instructions, using a Turner Biosystems luminometer.

Radio-labelling of mtDNA synthesis

α^{32}P-dCTP labelling of newly synthesised mtDNA in permeabilised cells was performed as described previously (Ashley *et al.*, 2007; Emmerson *et al.*, 2001).

siRNA transfections

For OPA1/p53/DRP1 knock-downs we used the previously validated siRNA sequences, 5′-GTTATCAGTCTGAGCCAGGdTdT-3′ for OPA1(Olichon *et al.*, 2003), 5'-GCAUGAACCGGAGGCCCAUdTdT-3' for p53 (Martinez *et al.*, 2002), and 5'-GCAGAAGAATGGGGTAAATdTdT -3' for Drp-1 (Griparic *et al.*, 2007). Qiagen AllStars siRNA was used as a negative control. 100 nM siRNA was tranfected using Dharmacon Dharmafect, as per manufacturer's protocols.

Immunoblotting

Was performed as described previously (Poulton *et al.*, 1994).

Statistical analysis

Statistical analysis was calculated using Microsoft Excel or SPSS. Significance was calculated using Student t-test.

Results

Doxorubicin and ethidium bromide alter nucleoid and mitochondrial morphology

To determine the long term effect of DXR on mtDNA we utilised PicoGreen fluorescence quenching to monitor DXR/DNA interactions within normal primary human fibroblasts, as described previously (Ashley and Poulton, 2009). In untreated cells nuclear and mtDNA were brightly labelled by PicoGreen (Fig. 1A i), and both signals were substantially quenched by addition of DXR, indicating intercalation of DXR into nuclear and mitochondrial DNA. Following 24 hours of DXR exposure PicoGreen fluorescence partially recovered in both the nucleus and mitochondria, the latter containing a small number of brightly labelled and grossly enlarged nucleoids. The average nucleoid diameter of these enlarged nucleoids was 1-3 μm, compared to ~ 0.8 μm of normal sized nucleoids. Although normally sized nucleoids remained within the DXR treated cell, they were often heavily quenched by DXR (t = 24h arrowed in inset). Hereafter, we term these DXR induced nucleoid alterations 'nucleoid remodelling'. Following DXR exposure, surviving cells allowed to recover in drug free medium for 72 hours displayed marked reduction in nucleoid PicoGreen labelling, despite recovery of the nuclear signal, suggestive of mtDNA depletion, which was confirmed using QPCR (Fig. 3D). Some remodelled nucleoids were still visible (arrowed)

Immuno-labelling of DXR treated fibroblasts with anti-DNA IgM (IgM1) capable of detecting nucleoids (Legros *et al.*, 2004) confirmed that DXR caused gross enlargement of nucleoids (Fig. 1A ii). The enlarged remodelled nucleoids appeared to be composed of aggregates of smaller nucleoids and there was noticeable clustering of nucleoids (arrowed), which was not generally seen in untreated cells. Co-labelling DXR treated fibroblasts with PicoGreen and the mitochondrial probe TMRM revealed mitochondria within DXR treated cells had undergone marked interlinking, with highly interconnected mitochondria (Fig. 1A iii and supplementary Figure 1B). Remodelled nucleoids frequently co-localised with small mitochondrial swellings not commonly observed in controls. Similar results were observed in DXR treated A549 cancer cells and H9C2 cardiomyocytes (supplementary Figure 1A and C), although H9C2s did not demonstrate mitochondrial interlinking (supplementary Figure 1D).

Anti-DNA and Mitotracker Red (which detects mitochondria in fixed cells) showed that ethidium bromide also caused marked nucleoid remodelling accompanied by mitochondrial interlinking (Figure 1A iv).

Quantification of a similar experiment to 1A showed that DXR could induce mitochondrial interlinking and remodelling at doses below 1 μM. H9C2 rat cardiomyocytes were more sensitive at low concentrations of DXR than human fibroblasts, but the level of remodelling was unaffected by incubating cells with the well known ROS scavenger *N*-acetylcysteine (Fig. 1B). DXR significantly reduced nucleoid numbers within individual fibroblasts (Fig. 1C), and significantly increased the average nucleoid fluorescence (Fig. 1D).

Remodelled nucleoids are enriched with TFAM, mtSSB and POLG

Within nucleoids, mtDNA is complexed with ‘core’ nucleoid proteins including mtSSB, POLG and TFAM, and associated, perhaps indirectly, with TID1 and ATAD3 (Bogenhagen *et al.*, 2008; He *et al.*, 2007). To determine if DXR affected these proteins, we immuno-labelled fibroblasts treated with DXR or vehicle. In untreated cells, TFAM was concentrated into small dots (nucleoids) distributed evenly along mitochondria, but was heavily concentrated into large mitochondrial blobs after DXR exposure (Fig. 2A). Large swathes of the mitochondria thus became depleted of detectable TFAM. The focal accumulations of TFAM co-localised with mitochondrial swellings, and with remodelled nucleoids (detected with anti-DNA IgM1 - not shown). Similar results were obtained using ethidium (not shown). Note that the strong red nuclear signal in DXR treated cells is due to auto-fluorescence of DXR intercalated into nuclear DNA, and was not due to Mitotracker. Mitochondrial DXR was not visible. Western blot of TFAM showed the total amount of TFAM remained un-affected by DXR treatment (Supplementary Fig. 2D).

Immuno-labelling of POLG1 (Fig. 2B) and mtSSB (supplementary Fig. 2C) also showed marked re-organisation into remodelled nucleoids in response to DXR treatment, although rarely as marked as TFAM. Lower camera exposure revealed that POLG enriched nucleoids consisted of small ‘dot like’ structures (Fig. 2B, *bottom panels*). Tid1 and ATAD3 showed re-localisation to a much lesser degree in response to DXR, but generally remained evenly distributed though-out mitochondria (supplementary figure 2A and B). Surprisingly, DXR

treatment substantially reduced the mtDNA binding affinity of a second anti-DNA antibody (IgM2) (Fig. 2C), suggesting a structural alteration to the mtDNA.

In conclusion, remodelled nucleoids were enriched with the core nucleoid proteins TFAM, mtSSB and POLG, and had reduced affinity for certain anti-DNA antibodies.

DXR inhibits mtDNA replication but remodelled nucleoids remain replicatively active

As DXR inhibits polymerases (Ellis *et al.*, 1987; Hixon *et al.*, 1981) we investigated the effect of DXR on DNA replication using α ^{32}P-dNTP labelling of permeabilised A549 cells (Emmerson *et al.*, 2001), which undergo remodelling and mitochondrial interlinking in response to DXR (supplementary Fig. 1A). DXR substantially reduced the amount of mtDNA α ^{32}P-dCTP incorporation relative to total mtDNA mass (determined with a total human mtDNA probe), indicating that DXR inhibited mtDNA replication (Fig. 3A *left*). Quantification of the bands showed a dose response effect, with a greater than 50% reduction of mtDNA synthesis after exposure to 3.4 μM DXR (Fig. 3A *right*). We also examined DNA synthesis in DXR treated fibroblasts using bromodeoxyuridine (brdU) labelling (Magnusson *et al.*, 2003). DXR and vehicle treated fibroblasts were incubated with brdU, and brdU labelled nuclear/mtDNA visualised with anti-brdU antibody. Measurements of the brdU intensity of S-phase nuclei and the number of brdU labelled nucleoids showed that DXR strongly inhibited nuclear synthesis, and sharply reduced the number of replicating nucleoids (Figure 3B). Most replicating nucleoids in DXR treated cells were enlarged i.e. re-modelled (Fig. 3C, *upper panels*). Since previous anti-DNA labelling had shown that numerous non-remodelled nucleoids remained within DXR treated cells (Fig. 1Aii), we determined if DXR had preferentially inhibited their replication, by double labelling DXR treated cells with brdU and anti-TFAM (Fig. 3C, *lower panels*). Within untreated cells, most TFAM positive nucleoids showed brdU labelling but within DXR treated cell only the largest remodelled nucleoids showed brdU incorporation comparable or greater than that of untreated nucleoids. A large number of non or partially remodelled nucleoids labelled by TFAM showed little or no brdU label (examples arrowed in insets).

To determine if DXR caused mtDNA depletion, we measured the total mtDNA copy number using quantitative real-time PCR (Fig. 3D). MtDNA levels were unaffected following a 24hour drug exposure, but showed a significant depletion of mtDNA after 48 hours, compared to controls. DXR was removed after 24 hours to reduce cellular toxicity but this did not alter the level of PicoGreen quenching (not shown), indicating DXR remained intercalated.

Thus, DXR preferentially inhibits mtDNA replication of non-remodelled nucleoids causing mtDNA depletion.

Nucleoid remodelling is not secondary to apoptosis and does not alter mitochondrial function

We next determined if remodelling preceded cell death or compromised mitochondrial dysfunction. Using TUNEL labelling we determined the cellular apoptotic index of DXR/vehicle treated (supplementary figure. 3A i). Following a 24-48 hour DXR exposure (3.4

μM), less than 10% of cells were apoptotic, well below the number of cells exhibiting remodelled nucleoids or increased mitochondrial interconnection. Calcein/propidium labelling showed less than 5% of the attached cell population were necrotic (supplementary Fig. 3A ii). DAPI/cytochrome c immuno-labelling showed no differences between vehicle and DXR treated cells, unlike cells treated with hydrogen peroxide, which showed nuclear located cytochrome c and chromosomal condensation (very bright DAPI signal), hallmarks of apoptosis (supplementary Fig. 3A iii). Remodelling did not occur during staurosporine-induced apoptosis (supplementary Fig. 3A iv). DXR did not significantly compromise mitochondrial function of fibroblasts or H9C2 cells, as determined by ATP generation, cellular oxygen consumption, cytochrome c oxidase histochemisty, and JC-1 fluorescence (supplementary Fig. 3B).

DXR induced nucleoid remodelling is mediated by OPA1 and mitofusin1 but not mitofusin 2

We next determined the influence of mitochondrial fusion on DXR induced remodelling by comparing wild-type mouse embryonic fibroblasts (MEFs) with mitochondrial fusion deficient MEFs harbouring null mutations in either MFN1 or MFN2 (Chen *et al.*, 2003). These MFN mutants contained fragmented mitochondria (supplementary Fig. 4A). Anti-DNA (IgM1) labelling indicated that whilst DXR induced substantial nucleoid remodelling within wild-type and MFN2 null MEFs, remodelling was almost totally suppressed within MFN1 null MEFs (Fig. 4A). Next we determined if OPA1 was also involved in nucleoid remodelling by ablating OPA1 levels in human fibroblasts using siRNA, confirmed by Western blot (supplementary Fig. 4B). DXR nucleoid remodelling, as detected by PicoGreen, was inhibited within the OPA1 siRNA transfected fibroblasts, but not in scramble siRNA transfected cells. Quantification showed that remodelling was almost totally suppressed by loss of OPA1 and MFN1, but not by loss of MFN2 (Fig. 4A, *graph*).

To determine if the suppression of nucleoid remodelling within MFN1 null cells led to increased sensitivity of mtDNA to DXR, we pulse-labelled wild-type, MFN1 and MFN2 MEFs with BrdU following a 24 hour treatment with DXR (1.7 μM). As shown in Figure 4D, mtDNA synthesis was markedly suppressed within MFN1 null cells, yet was well maintained by MFN2 and wild-type cells.

To determine if suppression of mitochondrial fission could alter nucleoids, we ablated DRP1 using siRNA. PicoGreen/TMRM co-staining showed that prolonged knock-down of DRP1 in fibroblasts lead to the formation of hyper-fused mitochondria, and large mitochondrial swellings which co-localised with apparently re-modelled nucleoids (Fig. 4C).

Collectively, the data above suggest that the nucleoid remodelling induced by DXR is mediated by MFN1 and OPA1, but not MFN2, and that suppression of remodelling renders mtDNA replication more susceptible to DXR inhibition. Furthermore nucleoid remodelling can be induced in the absence of DXR by inhibition of mitochondrial fission.

p53, ATM and POLG suppresses DXR induced remodelling

As DNA damage induced by DXR can trigger up regulation of p53 and its translocation to mitochondria where it is involved in mtDNA protection (Nithipongvanitch *et al.*, 2007a), we determined if altering p53 activity altered nucleoid remodelling. In DXR treated fibroblasts, p53 was up-regulated and this could be inhibited by p53 siRNA (Fig. 5A). Using PicoGreen we found that DXR remodelling was substantially increased by p53 knockdown (Fig. 5B). Chemical inhibition of p53 by pifithrin-α also increased remodelling confirming the specificity of the result. Remodelled nucleoids were larger and brighter in the p53 inhibited cells than in scramble or vehicle treated controls (Fig. 5B *lower*). As p53 activation by DXR is mediated mainly by ATM (Kurz *et al.*, 2004), we compared DXR remodelling in cells treated with either vehicle or the ATM inhibitor KU55933. ATM inhibition substantially increased the level of DXR remodelling (Fig. 5B).

To determine if the transcriptional activity of p53 was necessary for its influence on remodelling, we treated RH30 cells with DXR in the presence or absence of pifithrin-α, and counted the proportion of cells exhibiting strong nucleoid remodelling. RH30 cells express a mutant p53 protein unable to initiate transcription of p53 responsive genes (Felix *et al.*, 1992; McKenzie *et al.*, 2002). The amount of remodelling was increased by pifithrin-α treatment within RH30, suggesting p53 transcriptional activity was not required for the suppression of nucleoid remodelling (Fig. 5C).

To determine the influence of POLG exonuclease (proofreading) activity on DXR nucleoid remodelling we compared POLG wild-type and POLG exonuclease −/− MEFs derived from a trans-genetic knock-in mouse (Trifunovic *et al.*, 2004). POLG Exo −/− MEFs exhibited significantly more DXR induced nucelodi remodelling than identically treated wild-type controls (Fig. 5D).

In summary the data above indicates p53/ATM and POLG exonuclease activity suppresses DXR nucleoid remodelling.

DNA intercalators induce nucleoid remodelling

To determine the forms of DNA damage capable of triggering nucleoid remodelling we tested several drugs with known DNA damaging effects for their ability to induce remodelling, detected by either anti-DNA or PicoGreen labelling (Table 1). Certain anti-cancer drugs were found to induce varying levels of remodelling, including several anthracyclines, actinomycin D and ditercalinium. All compounds that induced remodelling were known DNA intercalators. Remodelling was not observed with specific inhibitors of topoisomerases, ROS generators, gamma radiation, DNA alkylating agents or nucleoside analogues, indicating DNA intercalation and not other forms of DNA damage triggered nucleoid remodelling.

Discussion

This study addresses the hypothesis that anti-cancer DNA intercalating drugs can directly affect mtDNA. We have previously shown that such drugs can rapidly intercalate into mtDNA of living cells (Ashley and Poulton, 2009). Here we show how these drugs

progressively alter the structure and arrangement of nucleoids and mitochondria, by causing nucleoid aggregation and mitochondrial interlinking. These effects were influenced by mitochondrial dynamics and ATM/ p53 activation, thereby showing mitochondrial nucleoids are linked to the genomic DNA damage response.

Within fibroblasts exposed to DXR, initial strong fluorescent quenching of PicoGreen by DXR showed that substantial intercalation occurred rapidly within nuclear and mtDNA (Fig. 1A), consistent with previous findings (Ashley and Poulton, 2009). However, after several hours, mtDNA fluorescence started to recover and was accompanied by the formation of giant, abnormally bright nucleoids, a process we describe as ‘nucleoid remodelling’. Although many non-remodelled nucleoids remained most failed to recover their fluorescence, indicating they lacked the ability to exclude DXR unlike their remodelled counterparts. Similar results were found within DXR treated H9C2 cardiomyocytes and A549 cancer cells. Anti-DNA labelling confirmed DXR exposed nucleoids were abnormal and showed ethidium also induced nucleoid alterations. Because these changes largely preceded DXR induced cell death, were not induced by staurosporine, and were induced by non-toxic doses of ethidium, we conclude that remodelling was not secondary to apoptosis.

TFAM became strongly enriched into remodelled nucleoids, and to a lesser extent mtSSB and POLG also. In contrast nucleoid proteins not believed to be directly bound to mtDNA such as ATAD3 and Tid1 showed much less alteration in their mitochondrial distribution. MtDNA binding by another anti-DNA IgM (IgM2) capable of detecting mtDNA was markedly reduced by DXR, suggesting nucleoid structure was altered so as to reduce its binding affinity. As IgM2 and IgM1 were raised against differing cellular epitopes, remodelling may alter the access of the antibodies to one but not the other epitope. α^{32}P-dCTP radiolabel and brdU incorporation showed mtDNA synthesis was significantly reduced by DXR (Fig. 3A) and DXR exposed cells consequently became depleted of mtDNA (Fig. 3D).

Remodelling was closely linked to mitochondrial dynamics as remodelling was accompanied by marked mitochondrial interlinking in certain cell types. Furthermore remodelling required the mitochondrial pro-fusion proteins MFN1 and OPA1 (Fig. 4), suggesting remodelling requires the aggregation of nucleoids from separate mitochondria. Remodelling did not require MFN2, which has a lower pro-fusion activity than that of MFN1 and is not essential for fusion (Chen *et al.*, 2005a; Cipolat *et al.*, 2004; Tondera *et al.*, 2009). DXR mediated mitochondrial interlinking may represent stress induced mitochondrial hyperfusion (SIMH), which has recently been shown to be a pro-survival response of cells treated with toxic agents (Tondera *et al.*, 2009). Notably we found that actinomycin D, which can induce SIMH, also triggers nucleoid remodelling (supplementary Fig. 2C), suggesting both phenomena are linked. Strikingly both SIMH and nucleoid remodelling similarly require OPA1 and MFN1, but not MFN2 activity. Mitochondrial fission may also play a role in nucleoid remodelling, as prolonged inhibition of fission via knock-down of DRP 1 caused the formation of highly interlinked mitochondria and enlarged nucleoids which co-localised with mitochondrial swellings (Figure 4C). However, immunoblotting failed to detect any DXR induced alterations of the expression of OPA1, DRP1, MFN2 or MFN2 (unpublished observations).

Nucleoid remodelling was specific to DNA intercalators, and not other forms of damage such as reactive oxygen species (table 1). DNA damage induced by DXR triggered the accumulation of p53 within the nuclei of treated cells, and inhibition of p53, or its upstream activator ATM, increased DXR nucleoid remodelling (Fig. 5B), indicating p53 repressed remodelling. Because this was apparently not due to p53s role as a transcription factor (Fig. 5C), it might well be due to its direct involvement in mtDNA protection. p53 can interact with POLG (Achanta et al., 2005), and is important for protecting mtDNA from damage by ethidium bromide (Achanta et al., 2005) and DXR (Nithipongvanitch et al., 2007b). POLG exonuclease null MEFs exhibited markedly increased remodelling compared to wild-type counterparts (Fig. 5D) indicating the proofreading exonuclease activity of POLG also suppresses nucleoid remodelling. Since p53 enhances POLGs exonuclease activity (Bakhanashvili *et al.*, 2009; Bakhanashvili *et al.*, 2008) p53 may exert its influence on nucleoid remodelling via its enhancement of POLG exonuclease activity.

In yeast, nucleoids can undergo structural alterations to protect mtDNA from damage during metabolic stress, possibly by allowing mtDNA to adopt a compact state (Chen *et al.*, 2005b; Kucej *et al.*, 2008). It is therefore conceivable that the ‘nucleoid remodelling’ we have characterised within mammalian cells helps to protect mtDNA from damaging intercalating agents. Several lines of evidence support this theory. Firstly, the absence of PicoGreen quenching by DXR within remodelled nucleoids shows they were more efficient at excluding DXR than non-remodelled nucleoids. Secondly, brdU/TFAM co-labelling demonstrated mtDNA synthesis was better maintained by large remodelled nucleoids than by smaller or non-remodelled nucleoids (Fig. 3C). Thirdly, mtDNA synthesis in the presence of DXR was markedly reduced within MFN1 null cells in which remodelling was suppressed, when compared to that of MFN2 null or wild type cells (Fig. 4A). This suggests that reducing nucleoid remodelling renders mtDNA more susceptible to DXR by, for example, increasing DXR intercalation. Finally, mitochondrial function was well maintained within DXR treated cells (supplementary Fig. 3) indicating remodelling did not compromise short term mitochondrial function as might be expected were the process pathogenic.

The present study and previous work (Ashley and Poulton, 2009), shows that mtDNA is a direct target for several clinically useful anti-cancer DNA drugs. This is consistent with the extensive mtDNA damage associated with human DXR pathology (Lebrecht *et al.*, 2005). Ethidium bromide, which had a similar affect on mtDNA as DXR, can trigger long-term mitochondrial dysfunction by damaging mtDNA (von Wurmb-Schwark *et al.*, 2006). Thus, *in vivo*, DXR intercalation into cardiac mtDNA and subsequent damage may contribute to the longer-term tissue dysfunction characteristic of DXR pathology.

Supplementary Material

Refer to Web version on PubMed Central for supplementary material.

Acknowledgements

We thank I. Sargent for use of equipment, E. Brampton, M. Zeviani, I. Holt, B. Roques, A.Trifunovic, P. Cook and D. Chan for materials, and K. Morten, and F. Brook for technical support. This work was funded by the MRC/ Wellcome Trust.

References

Abramoff MD, Magelhaes PJ, Ram SJ. Image Processing with ImageJ. Biophotonics International. 2004; 11:36–42.

Achanta G, Sasaki R, Feng L, Carew JS, Lu W, Pelicano H, et al. Novel role of p53 in maintaining mitochondrial genetic stability through interaction with DNA Pol gamma. EMBO J. 2005; 24:3482–92. [PubMed: 16163384]

Ashley N, Adams S, Slama A, Zeviani M, Suomalainen A, Andreu AL, et al. Defects in maintenance of mitochondrial DNA are associated with intramitochondrial nucleotide imbalances. Hum Mol Genet. 2007; 16:1400–11. [PubMed: 17483096]

Ashley N, Harris D, Poulton J. Detection of mitochondrial DNA depletion in living human cells using PicoGreen staining. Exp Cell Res. 2005; 303:432–46. [PubMed: 15652355]

Ashley N, O'Rourke A, Smith C, Adams S, Gowda V, Zeviani M, et al. Depletion of mitochondrial DNA in fibroblast cultures from patients with POLG1 mutations is a consequence of catalytic mutations. Hum Mol Genet. 2008; 17:2496–506. [PubMed: 18487244]

Ashley N, Poulton J. Mitochondrial DNA is a direct target of anti-cancer anthracycline drugs. Biochem Biophys Res Commun. 2009; 378:450–5. [PubMed: 19032935]

Bakhanashvili M, Grinberg S, Bonda E, Rahav G. Excision of nucleoside analogs in mitochondria by p53 protein. AIDS. 2009; 27:779–88. [PubMed: 19287302]

Bakhanashvili M, Grinberg S, Bonda E, Simon AJ, Moshitch-Moshkovitz S, Rahav G. p53 in mitochondria enhances the accuracy of DNA synthesis. Cell Death Differ. 2008; 15:1865–74. [PubMed: 19011642]

Bogenhagen DF, Rousseau D, Burke S. The layered structure of human mitochondrial DNA nucleoids. J Biol Chem. 2008; 283:3665–75. [PubMed: 18063578]

Chen H, Chomyn A, Chan DC. Disruption of fusion results in mitochondrial heterogeneity and dysfunction. J Biol Chem. 2005a; 280:26185–92. [PubMed: 15899901]

Chen H, Detmer SA, Ewald AJ, Griffin EE, Fraser SE, Chan DC. Mitofusins Mfn1 and Mfn2 coordinately regulate mitochondrial fusion and are essential for embryonic development. J Cell Biol. 2003; 160:189–200. [PubMed: 12527753]

Chen XJ, Wang X, Kaufman BA, Butow RA. Aconitase couples metabolic regulation to mitochondrial DNA maintenance. Science. 2005b; 307:714–7. [PubMed: 15692048]

Cipolat S, Martins de Brito O, Dal Zilio B, Scorrano L. OPA1 requires mitofusin 1 to promote mitochondrial fusion. Proc Natl Acad Sci U S A. 2004; 101:15927–32. [PubMed: 15509649]

Conklin KA. Coenzyme q10 for prevention of anthracycline-induced cardiotoxicity. Integr Cancer Ther. 2005; 4:110–30. [PubMed: 15911925]

Cullinane C, Cutts SM, Panousis C, Phillips DR. Interstrand cross-linking by adriamycin in nuclear and mitochondrial DNA of MCF-7 cells. Nucleic Acids Res. 2000; 28:1019–25. [PubMed: 10648796]

Ellis CN, Ellis MB, Blakemore WS. Effect of adriamycin on heart mitochondrial DNA. Biochem J. 1987; 245:309–12. [PubMed: 3663157]

Emmerson CF, Brown GK, Poulton J. Synthesis of mitochondrial DNA in permeabilised human cultured cells. Nucleic Acids Res. 2001; 29:E1. [PubMed: 11139631]

Felix CA, Kappel CC, Mitsudomi T, Nau MM, Tsokos M, Crouch GD, et al. Frequency and diversity of p53 mutations in childhood rhabdomyosarcoma. Cancer Res. 1992; 52:2243–7. [PubMed: 1559227]

Garrido N, Griparic L, Jokitalo E, Wartiovaara J, van der Bliek AM, Spelbrink JN. Composition and dynamics of human mitochondrial nucleoids. Mol Biol Cell. 2003; 14:1583–96. [PubMed: 12686611]

Griparic L, Kanazawa T, van der Bliek AM. Regulation of the mitochondrial dynamin-like protein Opa1 by proteolytic cleavage. J Cell Biol. 2007; 178:757–64. [PubMed: 17709430]

Hande KR. Clinical applications of anticancer drugs targeted to topoisomerase II. Biochim Biophys Acta. 1998; 1400:173–84. [PubMed: 9748560]

He J, Mao CC, Reyes A, Sembongi H, Di Re M, Granycome C, et al. The AAA+ protein ATAD3 has displacement loop binding properties and is involved in mitochondrial nucleoid organization. J Cell Biol. 2007; 176:141–6. [PubMed: 17210950]

Hixon SC, Ellis CN, Daugherty JP. Heart mitochondrial DNA synthesis: preferential inhibition by adriamycin. J Mol Cell Cardiol. 1981; 13:855–60. [PubMed: 7299833]

Jung K, Reszka R. Mitochondria as subcellular targets for clinically useful anthracyclines. Adv Drug Deliv Rev. 2001; 49:87–105. [PubMed: 11377805]

Kucej M, Kucejova B, Subramanian R, Chen XJ, Butow RA. Mitochondrial nucleoids undergo remodeling in response to metabolic cues. J Cell Sci. 2008; 121:1861–8. [PubMed: 18477605]

Kurz EU, Douglas P, Lees-Miller SP. Doxorubicin activates ATM-dependent phosphorylation of multiple downstream targets in part through the generation of reactive oxygen species. J Biol Chem. 2004; 279:53272–81. [PubMed: 15489221]

Lebrecht D, Kokkori A, Ketelsen UP, Setzer B, Walker UA. Tissue-specific mtDNA lesions and radical-associated mitochondrial dysfunction in human hearts exposed to doxorubicin. J Pathol. 2005; 207:436–44. [PubMed: 16278810]

Lebrecht D, Setzer B, Rohrbach R, Walker UA. Mitochondrial DNA and its respiratory chain products are defective in doxorubicin nephrosis. Nephrol Dial Transplant. 2004; 19:329–36. [PubMed: 14736955]

Legros F, Malka F, Frachon P, Lombes A, Rojo M. Organization and dynamics of human mitochondrial DNA. J Cell Sci. 2004; 117:2653–62. [PubMed: 15138283]

Magnusson J, Orth M, Lestienne P, Taanman JW. Replication of mitochondrial DNA occurs throughout the mitochondria of cultured human cells. Exp Cell Res. 2003; 289:133–42. [PubMed: 12941611]

Martinez LA, Naguibneva I, Lehrmann H, Vervisch A, Tchenio T, Lozano G, et al. Synthetic small inhibiting RNAs: efficient tools to inactivate oncogenic mutations and restore p53 pathways. Proc Natl Acad Sci U S A. 2002; 99:14849–54. [PubMed: 12403821]

McKenzie PP, McPake CR, Ashford AA, Vanin EF, Harris LC. MDM2 does not influence p53-mediated sensitivity to DNA-damaging drugs. Mol Cancer Ther. 2002; 1:1097–104. [PubMed: 12481433]

Nithipongvanitch R, Ittarat W, Velez JM, Zhao R, St Clair DK, Oberley TD. Evidence for p53 as Guardian of the Cardiomyocyte Mitochondrial Genome Following Acute Adriamycin Treatment. J Histochem Cytochem. 2007a

Nithipongvanitch R, Ittarat W, Velez JM, Zhao R, St Clair DK, Oberley TD. Evidence for p53 as guardian of the cardiomyocyte mitochondrial genome following acute adriamycin treatment. J Histochem Cytochem. 2007b; 55:629–39. [PubMed: 17312011]

Olichon A, Baricault L, Gas N, Guillou E, Valette A, Belenguer P, et al. Loss of OPA1 perturbates the mitochondrial inner membrane structure and integrity, leading to cytochrome c release and apoptosis. J Biol Chem. 2003; 278:7743–6. [PubMed: 12509422]

Poulton J, Morten K, Freeman-Emmerson C, Potter C, Sewry C, Dubowitz V, et al. Deficiency of the human mitochondrial transcription factor h-mtTFA in infantile mitochondrial myopathy is associated with mtDNA depletion. Hum Mol Genet. 1994; 3:1763–9. [PubMed: 7849699]

Singal PK, Iliskovic N. Doxorubicin-induced cardiomyopathy. N Engl J Med. 1998; 339:900–5. [PubMed: 9744975]

Steinherz L, Steinherz P. Delayed cardiac toxicity from anthracycline therapy. Pediatrician. 1991; 18:49–52. [PubMed: 1983861]

Suliman HB, Carraway MS, Ali AS, Reynolds CM, Welty-Wolf KE, Piantadosi CA. The CO/HO system reverses inhibition of mitochondrial biogenesis and prevents murine doxorubicin cardiomyopathy. J Clin Invest. 2007; 117:3730–41. [PubMed: 18037988]

Tokarska-Schlattner M, Wallimann T, Schlattner U. Alterations in myocardial energy metabolism induced by the anti-cancer drug doxorubicin. C R Biol. 2006; 329:657–68. [PubMed: 16945832]

Tondera D, Grandemange S, Jourdain A, Karbowski M, Mattenberger Y, Herzig S, et al. SLP-2 is required for stress-induced mitochondrial hyperfusion. EMBO J. 2009; 28:1589–600. [PubMed: 19360003]

Trifunovic A, Wredenberg A, Falkenberg M, Spelbrink JN, Rovio AT, Bruder CE, et al. Premature ageing in mice expressing defective mitochondrial DNA polymerase. Nature. 2004; 429:417–23. [PubMed: 15164064]

von Wurmb-Schwark N, Cavelier L, Cortopassi GA. A low dose of ethidium bromide leads to an increase of total mitochondrial DNA while higher concentrations induce the mtDNA 4997 deletion in a human neuronal cell line. Mutat Res. 2006; 596:57–63. [PubMed: 16488450]

Wallace KB. Doxorubicin-induced cardiac mitochondrionopathy. Pharmacol Toxicol. 2003; 93:105–15. [PubMed: 12969434]

Zhou S, Palmeira CM, Wallace KB. Doxorubicin-induced persistent oxidative stress to cardiac myocytes. Toxicol Lett. 2001; 121:151–7. [PubMed: 11369469]

Europe PMC Funders Author Manuscripts

Europe PMC Funders Author Manuscripts

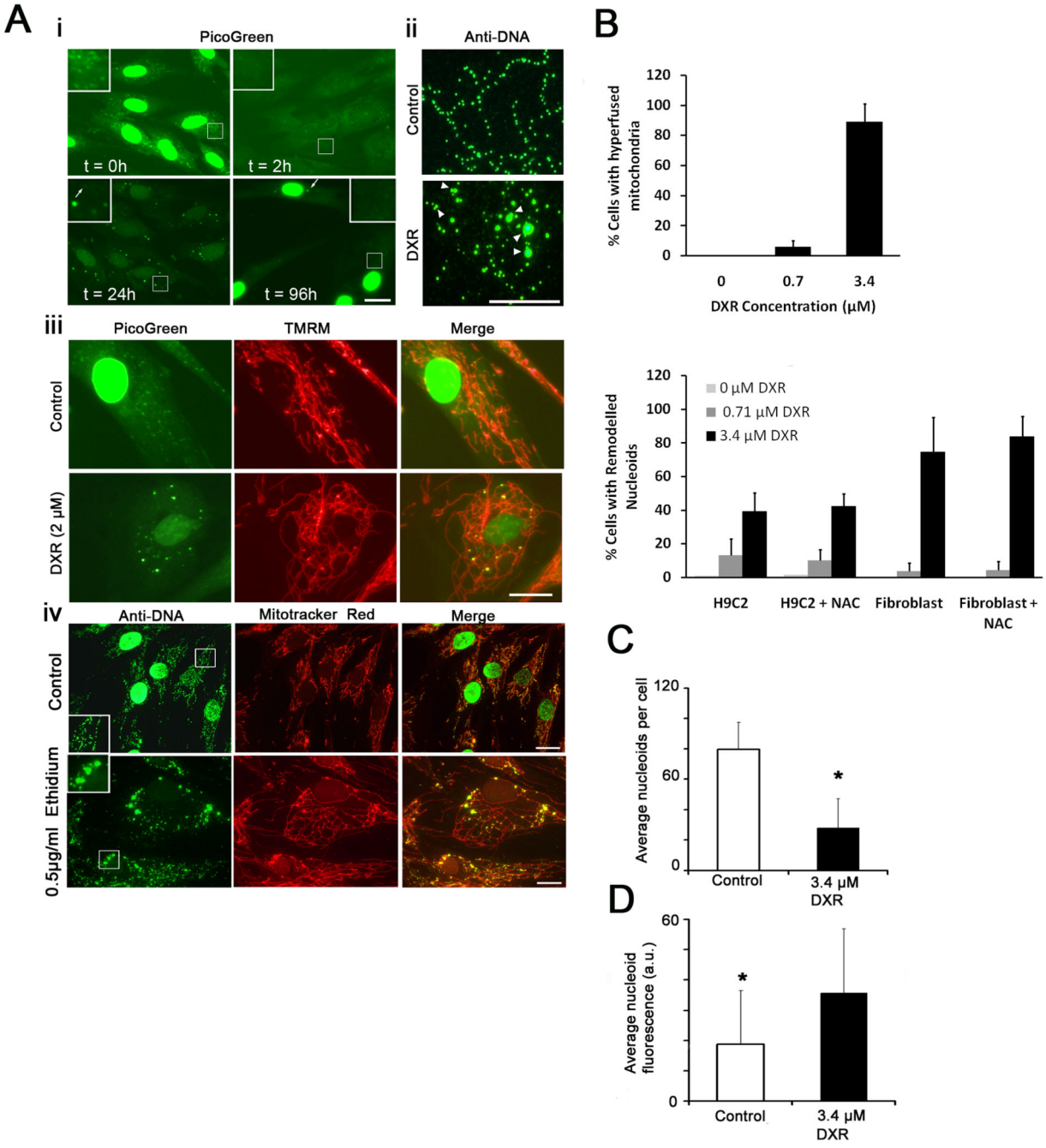

Figure 1.

DXR and ethidium alter mtDNA nucleoids and mitochondrial morphology. (Ai) Time-course of PicoGreen labelling of live primary human fibroblasts incubated with DXR (t = hours of exposure). (Aii) Anti-DNA (IgM1) labelling of mtDNA within DXR (3.4 µM 24 hours) and vehicle treated fibroblasts. (Aiii) PicoGreen/TMRM co-labelling of DXR/vehicle treated fibroblasts (2 µM 24 hours). (Aiv) Anti-DNA (IgM1)/Mitotracker red labelling of mtDNA/mitochondria within fibroblasts treated with vehicle or ethidium bromide (0.5µg/ml 24 hours). (B *upper*) Percentage of DXR/vehicle treated fibroblasts exhibiting mitochondrial

interlinking after 24 hours (n = 200). (B *lower*) Percentage of DXR/vehicle treated human fibroblasts and H9C2 rat cardiomyocytes exhibiting nucleoid remodelling after 24 hours, in the presence/absence of 100 μg/mL *N*-acetylcysteine (n = 200). (C) Mean nucleoids per cell within fibroblasts treated with DXR (3.4 μM 24 hours) or vehicle (n = 10). (D) Average nucleoid fluorescence (a.u. = arbitrary units) within fibroblasts treated with DXR/vehicle (3.4 μM 24 hours) (n = 100). * P = <0.05 versus control. Error bars + S.D. Results are representative of three independent experiments. Size bars: 20μm except Aii (10μm).

Europe PMC Funders Author Manuscripts

Europe PMC Funders Author Manuscripts

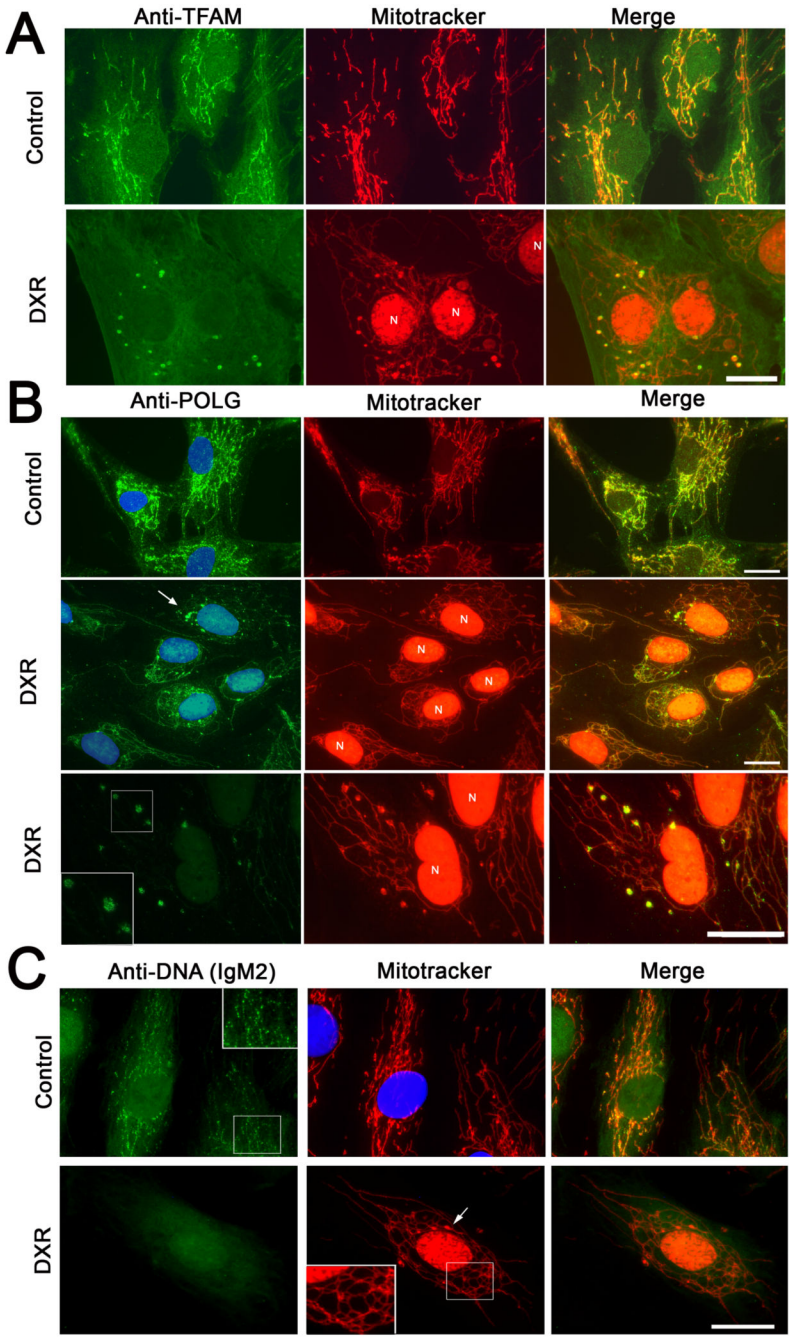

Figure 2.

DXR alters the distribution of TFAM, mtSSB and POLG and reduces mtDNA binding by Anti-DNA IgM2. (A) Anti-TFAM/Mitotracker labelling of fibroblasts incubated with vehicle/DXR (3.4 μM 24 hours). Retained DXR fluorescence within the nuclei is indicated by 'N'. (B) Anti-POLG/Mitotracker labelling of fibroblasts incubated with vehicle or DXR for 24 hours (3.4 μM 24 hours). DAPI was used to stain nuclei blue. DXR induced POLG accumulations are arrowed. The bottom panels show a higher magnification of a POLG labelling cell acquired using reduced camera exposure. (C) Anti-DNA IgM2/Mitotracker

labelling of fibroblasts incubated with vehicle/DXR (3.4 μM 24 hours). Arrow shows a mitochondrial swelling indicating a remodelled nucleoid. Size bars: 20μm. Results are representative of at least three independent experiments.

Europe PMC Funders Author Manuscripts

Europe PMC Funders Author Manuscripts

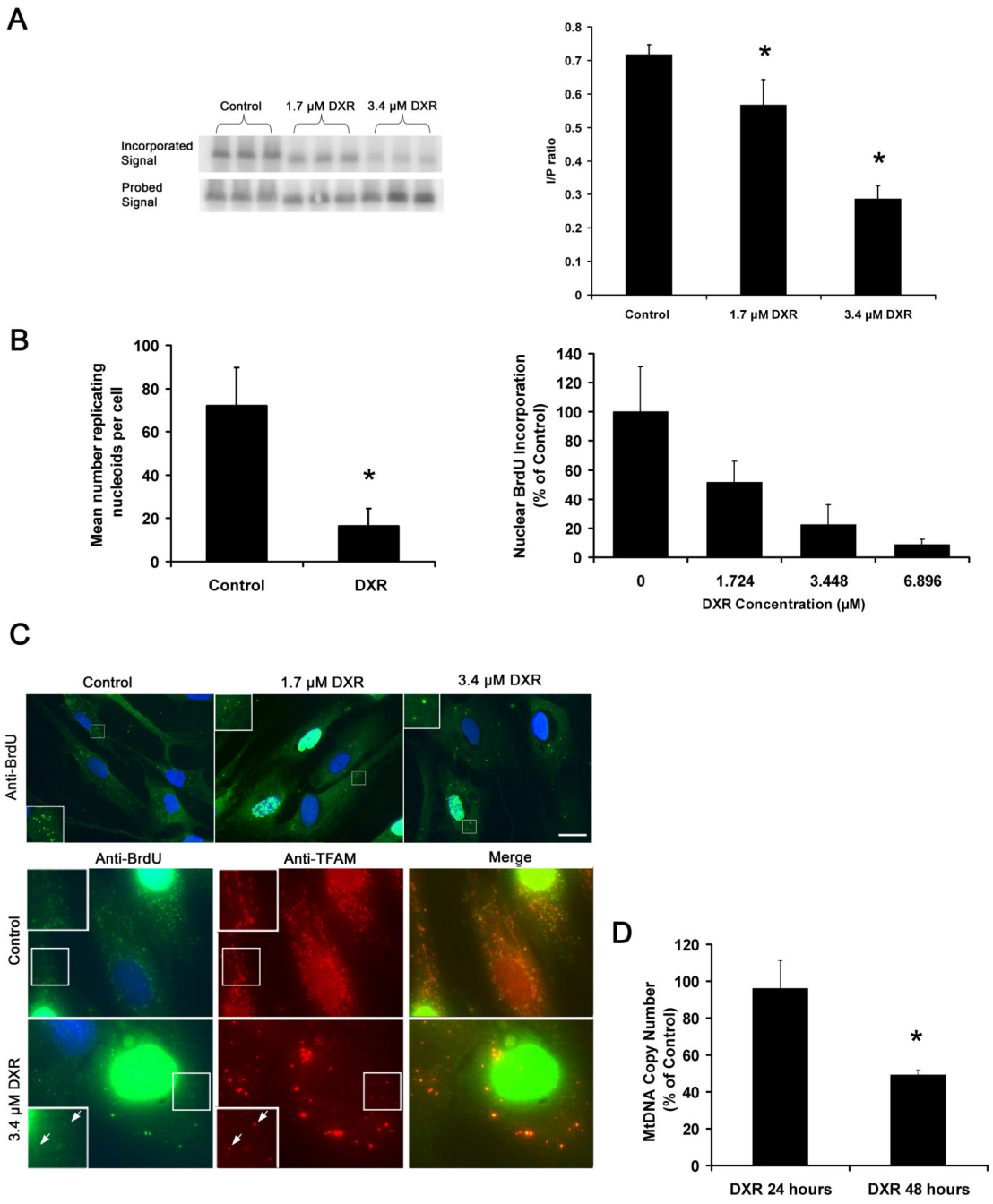

Figure 3.

DXR inhibits mtDNA synthesis and causes mtDNA depletion. (A) Phosphor-screen image of ^{32}P-dCTP incorporation of PVUII digested mtDNA, representing newly synthesised mtDNA, isolated from DXR/vehicle treated A549 (3.4μM DXR 24 hours), and the corresponding signal of the same mtDNA fragments hybridised to a total human mtDNA probe, representing the total mtDNA mass per lane. Graph shows quantification of the relative mtDNA fragment intensities (mtDNA replication) based on the mean of incorporated (I) vs probed (P) signal ratios (n = 3). (B *left*) Quantification of the average

number of brdU labelled (replicating) nucleoids of DXR/vehicle treated fibroblasts (3.4μM DXR 24 hours) (n = 100), following labelling with brdU (10 μM 6 hours), and immuno-detection by anti-brdU. (B *right*) Average nuclear brdU incorporation of S-phase cells from the same experiment (n = 100). (C *upper*) Image of brdU incorporation into cellular DNA of fibroblasts used to generate data for (B). DAPI was used to stain nuclei so S-phase nuclei appear white. (C *lower*) Anti-TFAM/brdU co-labelling of DXR/vehicle treated fibroblasts (3.4μM DXR 24 hours). (D) MtDNA to nuclear DNA ratios of fibroblasts treated with vehicle/DXR (1.7 μM) for up to 48 hrs, as determined by real-time quantitative PCR (n = 3). Note that the drug was washed out after 24 hours to reduce cellular toxicity. This had no effect on nucleoid remodelling or PicoGreen quenching (not shown). * P = <0.05. Error bars +S.D. Size bars: 20μm. Results are representative of three independent experiments.

Europe PMC Funders Author Manuscripts

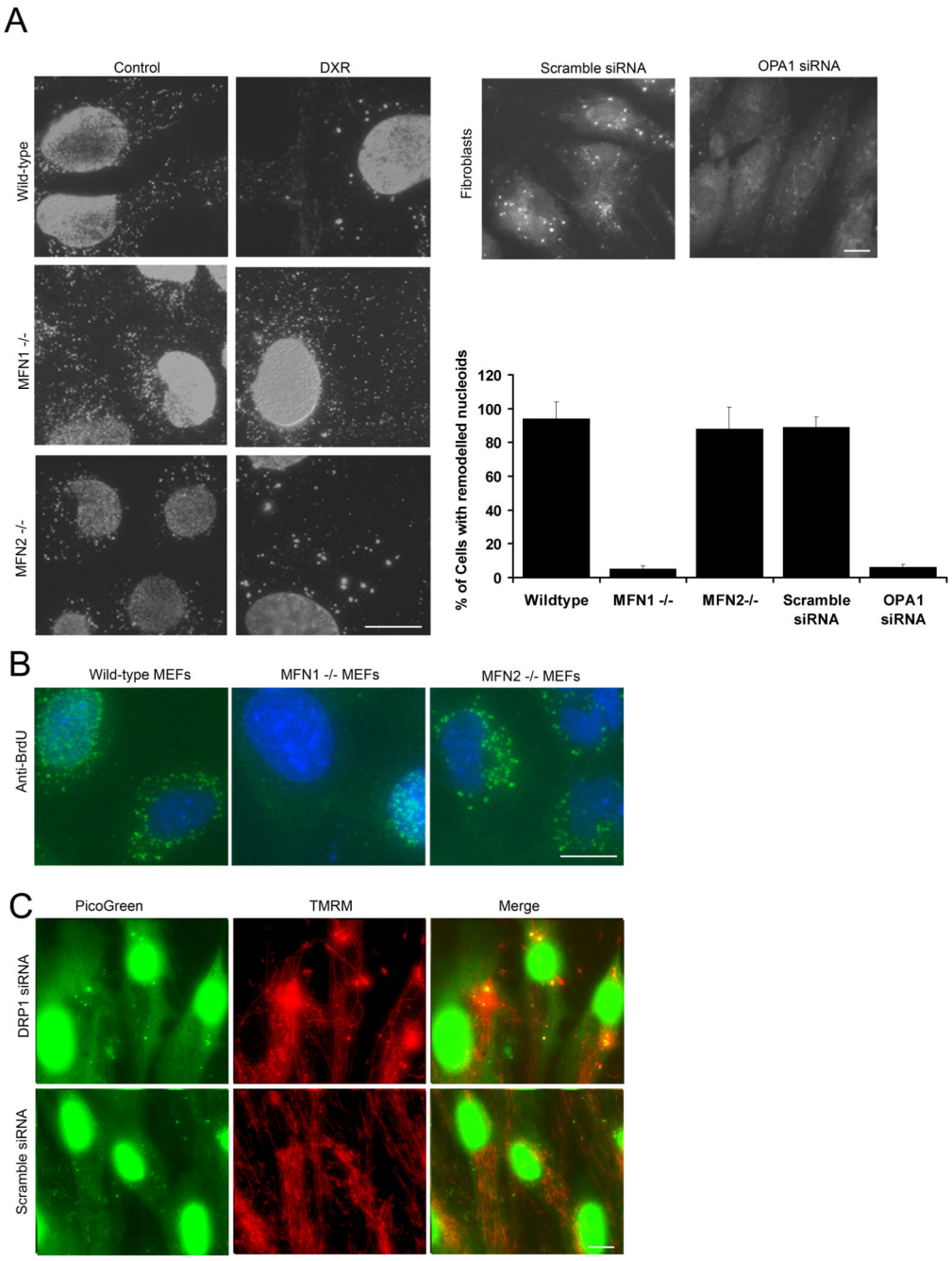

Figure 4.

Influence of MFN1/2,OPA1 and DRP1 on DXR induced nucleoid remodelling. (A *left*) Anti-DNA IgM1 labelling of DXR/vehicle treated wild-type, MFN1 null and MFN2 null MEFs (7.2 μM DXR 24 hrs). (A *right*) PicoGreen labelling of fibroblasts transfected with either OPA1 targeting siRNA (48 hours) or a scramble siRNA control, after treatment with DXR (7.2 μM 24 hours). (A *graph*) Quantification of % cells with DXR induced remodelled nucleoids (n = 200). (B) Representative brdU labelling (20μM 24 hours) of wild-type, MFN1 and MFN2 null cells, treated with vehicle/DXR (3.4 μM 24 hours). (C) PicoGreen/

TMRM labelling of DRP1/Scramble siRNA treated cells (6 days). Bars 20 μm. Results + S.D. Results are representative of three independent experiments.

Europe PMC Funders Author Manuscripts

Europe PMC Funders Author Manuscripts

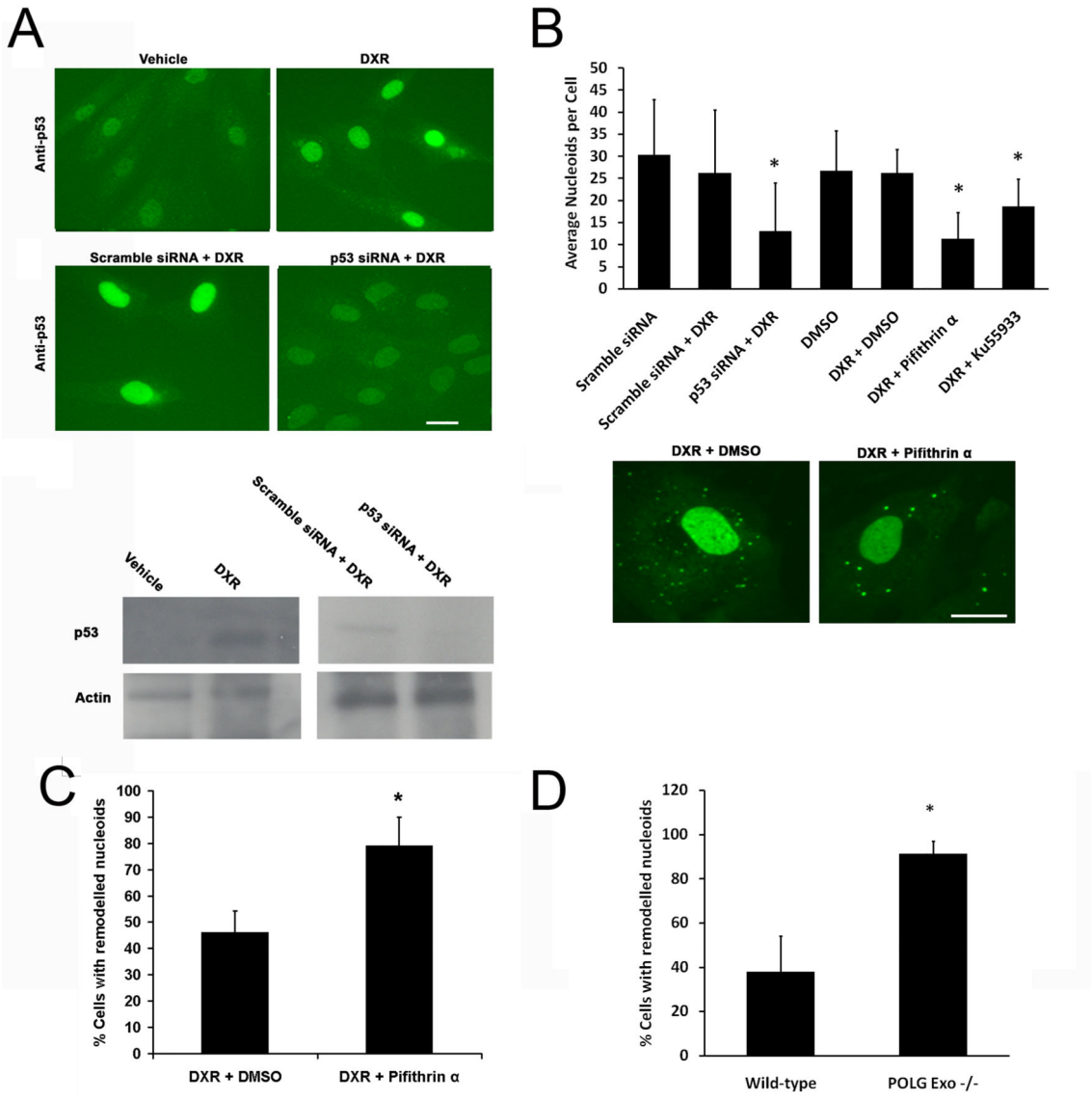

Figure 5.

p53, ATM and POLG suppress DXR induced nucleoid remodelling. (A *upper panel*) Anti-p53 immuno-labelling of fibroblasts treated with vehicle or DXR (1.7 μM for 24 hours) or transfected with p53/control, following exposure to 3.4 μM DXR for 24 hours. (A *lower*) Immuno-blot of similar experiment to A. (B *upper panels*) Quantification of nucleoid remodelling of DXR treated (3.4 μM 24 hours) fibroblasts in which p53 was inhibited by siRNA or pifithrin-α (10 μg/ml), or ATM inhibited by KU55933 (10 μM) (n = 20). (B *lower panels*) Typical PicoGreen staining of cells treated with DXR in the presence of vehicle or

pifithrin-α. (C) Effect of vehicle or pifithrin-α (10 μg/ml) on DXR (3.4 μM 24 hours) induced nucleoid remodelling in RH30 cells expressing a p53 transcription mutant (n = 20). (D) Nucleoid remodelling exhibited by wild-type or POLG exonuclease null MEFs treated with DXR (3.4 μM 24 hours) (n =100). Results +S.D. *P <0.05. Bars 20μm. Results are representative of three independent experiments.

Europe PMC Funders Author Manuscripts

Table 1

Compounds tested for ability to induce nucleoid remodelling in Fibroblasts. Cells were incubated with medium containing compounds at the specified concentrations for 24 hours, and nucleoid remodelling detected with PicoGreen.

Drug/Process	Tested Concentration	Physiological Effect	Nucleoid remodelling inducer
Doxorubin (Anthracycline)	0.7 – 7.5 μM	DNA intercalator, topoisomerase II inhibitor^{+}	Yes
Daunorubicin (Anthracycline)	0.5 – 3.4 μM	DNA intercalator, topoisomerase II inhibitor^{+}	Yes
Epirubicin (Anthracycline)	0.5 – 3.4 μM	DNA intercalator, topoisomerase II inhibitor^{+}	Yes
Idarubicin (Anthracycline)	0.5 – 3.4 μM	DNA intercalator, topoisomerase II inhibitor^{+}	Yes
Aclarubicin (Anthracycline)	1.7 – 3.4 μM	DNA intercalator, topoisomerase II inhibitor$^{\$}$	Yes
Ethidium bromide	0.5 – 1μg/ml	DNA intercalator	Yes
Actinomycin D	5 – 10μM	DNA intercalator, topoisomerase inhibitor^{+}	Yes
Ditercalinium	0.5 – 1 μg/ml	DNA intercalator, topoisomerase inhibitor$^{\$}$	Yes
Etoposide	10 - 20 μM	Topoisomerase II inhibitor$^{\$}$	No
Ciprofloxacin	10 – 50 μM	Topoisomerase II inhibitor^{+}	No
Sobzuzoxane	50 – 100 μM	Topoisomerase II inhibitor$^{\$}$	No
Campthofecin	10 -20 μM	Topoisomerase I inhibitor	No
ICRF-193	50 - 100 μM	Topoisomerase II inhibitor$^{\$}$	No
Cisplatin	10 – 50 μM	DNA cross-linker	No
Bleomycin	50 μg/ml	DNA damager	No
Hydroxyurea	0.5 - 1 mM	Ribonucleotide reductase inhibitor	No
Menadione	5 - 10 μM	Mitochondrial ROS generator	No
Bromodeoxyuridine	10-20 μM	Nucleoside analogue	No
Dideoxycytidine	5 - 15 μM	Nucleoside analogue	No
Gamma irradiation	3000 Rad	DNA damager	No
Chloramphenicol	25-50 μg/ml	Mitochondrial translation inhibitor	No
Xanthine/Xanthine oxidase	50 U	ROS generator	No
H_2O_2	200-500 mM	ROS generator	No

Key:

$^{\$}$Catalytic inhibitor

$^{+}$Poison